Implications of the Mullins Effect on the Stiffness of a Pre-loaded Rubber Component

Ryan E. Paige, Will V. Mars

Cooper Tire & Rubber Company

Abstract: Many engineered rubber components are pre-loaded during manufacture or installation in such a way that the rubber experiences compressive loads that are partially relieved during operation. In this paper, we investigate the consequences of applying this type of loading when the rubber exhibits a Mullins effect. The Mullins effect is a dependence of the hyperelastic response on the maximum deformation previously experienced. ABAQUS contains a new model for this effect, and we first examine the significance of the model parameters. Then we show that the total stiffness of a rubber component may either decrease or increase significantly by including the Mullins effect. To do this, we compare computed load-deflection curves for the cases of a) a purely hyperelastic material, and b) a material having identical monotonic behavior as the hyperelastic material, but exhibiting the Mullins effect. The possibility of increased component stiffness at first seems counterintuitive, but has a simple explanation. It is thus shown necessary to consider the Mullins effect when modeling load deflection response of rubber components since there are cases where it may significantly increase the accuracy of a prediction.

Keywords: Hyperelasticity, Rubber, Vibration, Mullins Effect and NVH Automotive Components.

1. Introduction

Rubber components are widely used in vibration control engineering applications due to their versatility and inherent physical characteristics. Particularly important are the ability to withstand large strains, and their intrinsic damping behavior. In the automotive noise, vibration and harshness (NVH) system control industry these parts are conventionally developed with natural rubber and are typically categorized as bushings, jounce bumpers and shock, strut, body, cradle and engine mounts. Many of these parts are designed to include a *pre-compression*, which is a compressive pre-load that is applied during manufacture or installation. The amount of pre-compression may vary widely, from minor swaging of a bushing to eliminate residual thermal stresses incurred during the molding process, to large amounts intended to keep the rubber in compression throughout its loading history.

Two common types of mounts in the automotive industry involve essentially two independent sections of rubber, each of which is subjected to relatively large amounts of pre-compression.

These are often referred to as the clam shell mount, typically used as a powertrain isolator, and the split shell mount, often used as cradle mount (see Figures 1 and 2). Applying pre-compression during assembly subjects the rubber to large stresses that can change the subsequent material response via the Mullins effect. The consequences of this on the initial static stiffness response of a component are investigated herein.

2. The Mullins Effect

2.1 Phenomenology

The stress-strain response in filled rubbers typically depends strongly on the maximum loading previously encountered. The phenomenon is widely known as the Mullins effect. Mullins (Mullins, 1969) studied the transient stress-strain response of rubber under cyclic loading. On the initial loading, he found the virgin material exhibits a relatively stiff response. When the material is subsequently unloaded, then reloaded, the stress-strain curve follows a significantly softer path. After several cycles, the stress-strain response stabilizes, and additional cycles merely retrace the path of the stabilized stress-strain curve. If the previous maximum strain is not exceeded, the effect is relatively permanent (Mars and Fatemi, 2004).

Figure 3 illustrates this effect for a typical compound. These particular results were generated in simple tension. Monotonic and cyclic stress-strain curves are plotted. A new specimen was used to generate the monotonic data. Another new specimen was then used to generate the cyclic curves, at 3 different levels of maximum strain, in order from the lowest level of maximum strain to the highest. The cyclic curves are plotted for the 8th cycle. It can be seen that the cyclic curves are significantly softer than the monotonic curve, by an amount depending on the maximum strain experienced. The higher the maximum strain, the softer the response.

2.2 Material model

The Mullins effect can be idealized for many purposes as an instantaneous and irreversible softening of the cyclic stress-strain curve relative to the stress-strain curve that would occur during monotonic loading of a new specimen. Softening occurs whenever the load increases beyond its prior all-time maximum value. At times when the load is less than a prior maximum, nonlinear elastic behavior prevails. The model does not address inelastic effects associated with set, creep, or hysteresis. It does not address the dependence of dynamic stiffness on dynamic strain amplitude (sometimes called the Payne effect or the Fletcher/Gent effect).

ABAQUS version 6.4 offers a material model (via the *MULLINS keyword) based on the idealization described above (Bose et al, 2003). The model is based on the work of Ogden and Roxburgh (Ogden and Roxburgh, 1999). As in hyperelasticity, their model derives from an energy density function, albeit one that exhibits history dependence under certain conditions. The energy function is written in terms of the invariants I_1 and I_2 of the isochoric Green deformation tensor $\mathbf{C} = (\det \mathbf{F})^{-2/3} \mathbf{F}^{\mathbf{T}}\mathbf{F}$. The energy function has the form

$$W(I_1, I_2, \eta) = \eta \bar{W}(I_1, I_2) + \phi(\eta) \qquad (1)$$

where

W is the deviatoric part of the strain energy function of the material.

$\tilde{W}$ is the deviatoric strain energy function that arises by regarding the stress-strain curve resulting from monotonic loading of the material (prior to any preconditioning) as non-linear elastic. Herein, the stress-strain curve associated with this energy function will be called the *primary* stress-strain curve, following Ogden and Roxburgh. The maximum value of $\tilde{W}$ achieved in all prior history is denoted $\tilde{W}_{\max}$.

ϕ is a smooth function of η complying with the conditions that $-\phi'(\eta) = \tilde{W}(I_1, I_2)$ and $\phi(1) = 0$. Ogden and Roxburgh call this the *damage function.* When the damaged material is in the undeformed state, the energy function has a residual value of $W = \phi(\eta(\tilde{W}_{\max}))$. This quantifies the non-recoverable energy that corresponds to the area between the initial monotonic stress-strain curve, and the particular stress-strain curve along which unloading occurs.

η is defined by

$$\eta = \begin{cases} 1 & \text{if } \tilde{W}(t) \geq \tilde{W}(s) \text{ for all } s : 0 < s < t \\ 1 - \dfrac{1}{r}\operatorname{erf}\left[\dfrac{\tilde{W}_{\max} - \tilde{W}}{m + \beta \tilde{W}_{\max}}\right] & \text{if } \tilde{W}(t) < \tilde{W}(s) \text{ for any } s : 0 < s < t \end{cases} \qquad (2)$$

where r, m, and β are material parameters. Note that the particular damage function η applied herein differs slightly from the function originally proposed by Ogden and Roxburgh (Bose et al, 2003). However, their model can be recovered from this model by taking $\beta = 0$.

The monotonic Cauchy stress ("true" stress) calculation is given by:

$$\boldsymbol{\sigma} = 2\,\mathrm{dev}\left[\left(\frac{\partial \tilde{W}}{\partial I_1} + I_1 \frac{\partial \tilde{W}}{\partial I_2}\right)\bar{\mathbf{B}} - \frac{\partial \tilde{W}}{\partial I_2}\bar{\mathbf{B}} \cdot \bar{\mathbf{B}}\right] - p\mathbf{I} \qquad (3)$$

where dev(**A**) = **A** - tr(**A**)/3 denotes the deviatoric part of the argument tensor, p is the hydrostatic pressure (compression being taken as positive), **I** is the identity tensor, and

$$\bar{\mathbf{B}} = \mathbf{F}\mathbf{F}^T. \qquad (4)$$

F is the deformation gradient, satisfying det(**F**) = 1.

The Cauchy stress after pre-conditioning is given by

$$\boldsymbol{\sigma} = 2\eta\,\mathrm{dev}\left[\left(\frac{\partial \bar{W}}{\partial I_1} + I_1\frac{\partial \bar{W}}{\partial I_2}\right)\bar{\mathbf{B}} - \frac{\partial \bar{W}}{\partial I_2}\bar{\mathbf{B}}\cdot\bar{\mathbf{B}}\right] - p\mathbf{I} \qquad (5)$$

2.3 Physical meaning of model parameters

Although the Ogden-Roxburgh model is purely phenomenological in nature, its parameters are related to particular physical aspects of the stress-strain response. To see this, note first that at a given deformation state in plane stress, the function η corresponds to the ratio of the softened stress to the stress on the primary curve. See Figure 4. Note that as the material configuration varies from the undeformed state to a state that reaches the all-time maximum primary strain energy density $\bar{W}_{\max}$, the ratio η varies from an initial value in the range $0 < \eta < 1$ to a final value of $\eta = 1$.

The function η depends both on the instantaneous strain energy density $\tilde{W}$, and on the maximum-ever strain energy density $\bar{W}_{\max}$. Figure 5 shows the variation of η with $\tilde{W}$, for typical values of the material parameters. Each curve shown represents a different value of $\bar{W}_{\max}$.

The significance of the material parameters *r*, *m*, and β can be established by considering several limiting cases of the model. First, consider the case that $\bar{W}_{\max} \to \infty$ at the same time that $\bar{W} \to 0$. This provides a measure of how much softening occurs at small strains, following the application of preconditioning at a very severe strain. If (as in the original Ogden-Roxburgh model) $\beta = 0$, then the value of the erf function in equation (2) quickly approaches 1. For all practical purposes, this also happens if $\beta \le 1/2$. *For these cases, the parameter r is readily identified as the reciprocal of the largest fraction by which the material can possibly be softened,* as shown in Figure 5. When $\beta > 1/2$, the limit as $\bar{W}_{\max} \to \infty$ comes to depend both on β and *r*, ie $\eta \to 1 - \frac{1}{r}\,\mathrm{erf}(\beta^{-1})$. Note that as $\beta \to \infty$, $\mathrm{erf}(\beta^{-1}) \to 0$, implying that little or no softening will occur. To avoid dependence of this limit on β, it may be desirable to enforce the constraint that $\beta \le 1/2$.

Next consider what happens as the ratio $\bar{W}/\bar{W}_{\max}$ varies over the range $0 \le \bar{W}/\bar{W}_{\max} \le 1$, with $m > 0$. If $\bar{W}_{\max} << m$, then the erf function evaluates nearly to zero, and little softening is predicted. On the other hand, if $\bar{W}_{\max} >> m$, then the erf function evaluates nearly to one, and the maximum amount of softening (defined by *r*) occurs. The effect is illustrated both in Figure 5 and in Figure 6. Thus, *the parameter m may be viewed as the strain energy density, associated with the primary curve, at which the maximum amount of softening is first achieved.*

In Figure 6, $\beta = 0$, as in the original model of Ogden and Roxburgh. For large values of $\bar{W}_{\max}$, this choice for β may lead to convergence difficulties in a finite element analysis upon unloading of the material, due to the large change in tangent stiffness. Comparing Figures 5 and 6 suggests that the effect of the parameter β is to limit this change. This can be confirmed by computing the derivative $\partial\eta / \partial\bar{W}$, which turns out as

$$\frac{\partial \eta}{\partial \bar{W}} = \frac{2}{r\sqrt{\pi}(m + \beta \bar{W}_{\max})} \exp\left[-\left(\frac{\bar{W}_{\max} - \bar{W}}{m + \beta \bar{W}_{\max}} \right)^2 \right] \qquad (6)$$

In the limit as $\bar{W} / \bar{W}_{\max} \to 1$, and for $\bar{W}_{\max} >> m$, this becomes simply

$$\frac{\partial \eta}{\partial \bar{W}} = \frac{2}{r\sqrt{\pi}\beta \bar{W}_{\max}} \qquad (7)$$

Thus, *the parameter β may be viewed as governing the slope of the softening curve, at the point where the primary and softened curves join (ie at $\bar{W} / \bar{W}_{\max} = 1$),* for large $\bar{W}_{\max}$.

It is important to note that the parameter *m* should not be taken as zero. The choice *m* = 0 would imply that Mullins softening occurs at arbitrarily small strains, which is not physically realistic. This behavior is illustrated in Figure 7.

2.4 Material characterization

For the analyses reported in the remainder of this work, the Mooney-Rivlin model was used to represent the primary curve. A comparison of this model with corresponding experimental results in simple, planar, and equibiaxial tension is shown in Figure 8. Note that the ability of the Ogden-Roxburgh model to capture softened behavior depends firstly on an adequate model for the primary stress-strain behavior.

The parameters of the Ogden-Roxburgh model for the Mullins effect were obtained via a nonlinear least squares scheme. An example of stress-strain curves measured following various levels of preconditioning compared to model predictions is shown in Figure 9. This data was collected in planar tension. A reasonable fit is obtained.

3. Component stiffness predictions in the presence of pre-compression

In this section, we compare computed load-deflection curves for the following cases: a) a purely hyperelastic material, and b) a material having identical monotonic behavior as the hyperelastic material, but exhibiting the Mullins effect. We will see that the stiffness of a rubber component

may either decrease or increase as a result of including Mullins effect. The latter possibility at first seems counter-intuitive, but has a simple explanation.

3.1 Split shell mount details

Split shell isolators like the one shown in Figure 2 are often used for light vehicle cradle mounts. A cut-away view of the rubber element is seen on the left. In Figure 10, the two separate outer shell surfaces and inner metal surface are highlighted. These rubber regions are bonded to metal and are treated as rigid. The mount is assembled by pressing it into a housing, forcing the two split outer shells together and pre-compressing the rubber elements. The assembled state is shown on the right in Figure 2, and for this case the symmetric sections of rubber are subjected to roughly 25% pre-compression. The inner metal rigid body is then loaded via displacement control in the radial direction while the outer shells are held fixed. This load case increases compression in one rubber section while unloading, or decreasing the compression in the other section of rubber.

3.2 Split shell model results and discussion

Identical numerical methodology is used to compare predictions for the cases of a) no Mullins effect (purely hyperelastic), and b) Mullins effect turned on. First, considering only the assembly stage for ½ of the split shell mount, Figure 11 compares resulting force deflection curves for pre-compression loading and unloading. Note that the behavior is analogous to the behavior exhibited by the material - i.e. on unloading, the response is softer. We would also expect that the larger the maximum deformation, the larger the degree of softening that occurs on unloading.

Figure 12 compares load deflection curves for the whole split shell mount, for these cases a) no Mullins effect, b) Mullins effect turned on. Assembly of the component results in both halves supporting a compressive load. Subsequent to assembly, positive displacement of the center piece of the component causes unloading on one side of the mount, and increased compressive loading on the other side of the mount. Note how the total response becomes stiffer.

To better understand how this can happen, it is helpful to consider the loading in each half of the mount. The time history of the load is plotted in Figure 13. It can be seen that when the Mullins effect is active, the decreased compressive load on the side of the mount that is unloading causes the total reaction at the center piece to increase. Consider also the recoverable energy in the model. Figure 14 shows the dissipation that occurs due to the activation of the Mullins effect by comparing the recoverable energy with the Mullins effect activated and for the purely hyperelastic case. After pre-compression, as the inner metal is loaded, the compressed rubber section that is unloaded has less recoverable strain energy to release, requiring more external energy to be applied to further compress the opposite rubber section.

3.3 A final example: Severe loading of a clamshell mount

Although the Mullins effect occurs rapidly with the first few high-severity loading events, it can significantly influence the subsequent long-term behavior of a rubber component (Mars & Fatemi, 2004). The dependence of the stress-strain response on pre-conditioning implies that each material point in a non-homogeneously strained component exhibits a distinct stress-strain behavior. Although all such points may behave more or less in accordance with a hyperelastic

law, the particular hyperelastic law varies from point to point. Because of this, a single hyperelastic law for all material points is unlikely to give realistic predictions. By including the Mullins effect, it is possible to accurately model loading and unloading events.

The clamshell mount in this final example exhibits some very difficult aspects for predicting behavior of a natural rubber component. Referring back to Figure 1 it can be seen that the upper and lower rubber sections are not symmetric. The two rubber sections have different volumes, heights and overall shape. Furthermore, the pre-compression is large (greater than 25%). In one continuous loop the inner metal is subjected to very large working loads in both the positive and negative vertical directions. However, with the incorporation of the Mullins effect, very good correlation can be achieved between the predicted response and experiment. Figure 15 compares load deflection curves for prediction and experiment, and Figure 16 shows the deformed shapes.

4. Conclusion

The significance of the parameters r, m, and β of the Ogden-Roxburgh model was investigated. The parameter r was identified as the reciprocal of the largest fraction by which the material can possibly be softened (when $\beta \le 1/2$). The parameter m was found to be associated with the strain energy density on the primary curve at which the maximum amount of softening is first achieved. The parameter β may be viewed as governing the slope of the softening curve, at the point where the primary and softened curves join.

The total stiffness of a rubber component may either decrease or increase as a result of including the Mullins effect. The latter possibility at first seems counterintuitive, but was shown to be a consequence of different amounts of softening occurring on each side of the pre-loaded mount. It is thus necessary to consider the Mullins effect when modeling load deflection response of rubber components since there are cases where it may significantly increase the accuracy of a prediction.

5. References

Bose, K, Hurtado, J.A., Snyman, M. F., Mars, W. V., Chen, J. Q., "Modelling of stress softening in filled elastomers," Constitutive Models for Rubber III, pp. 223-230, Busfield and Muhr (eds), Swets & Zeitlinger, Lisse, 2003.

Mars, W. V., Fatemi, A., Observations of the Constitutive Response and Characterization of Filled Natural Rubber under Monotonic and Cyclic Multiaxial Stress States, Journal of Engineering Materials and Technology, Vol. 126, Issue 1, pp. 19-28, 2004.

Mullins, L., "Softening of Rubber by Deformation," Rubber Chemistry and Technology, Vol. 42, pp. 339-362, 1969.

Ogden, R. W., Roxburgh, D. G., "A pseudo-elastic model for the Mullins effect in filled rubber," Proceedings of the Royal Society of London, A, Vol. 455, pp. 2861-2877, 1999.

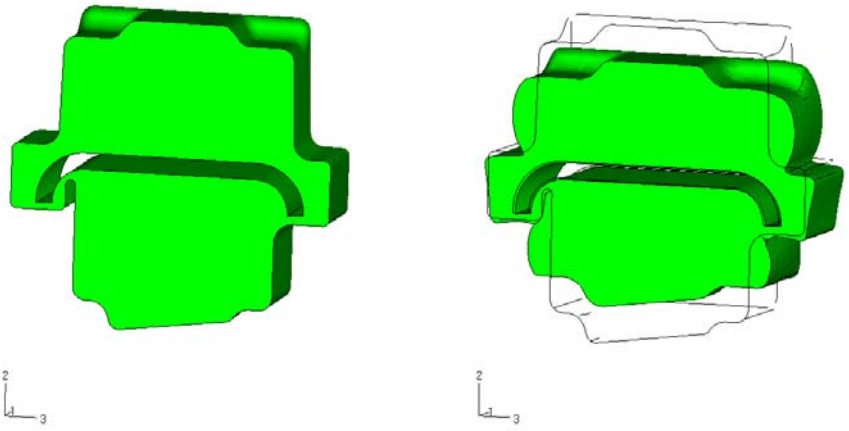

Figure 1. Clam shell mount as molded (left) and after assembly (right).

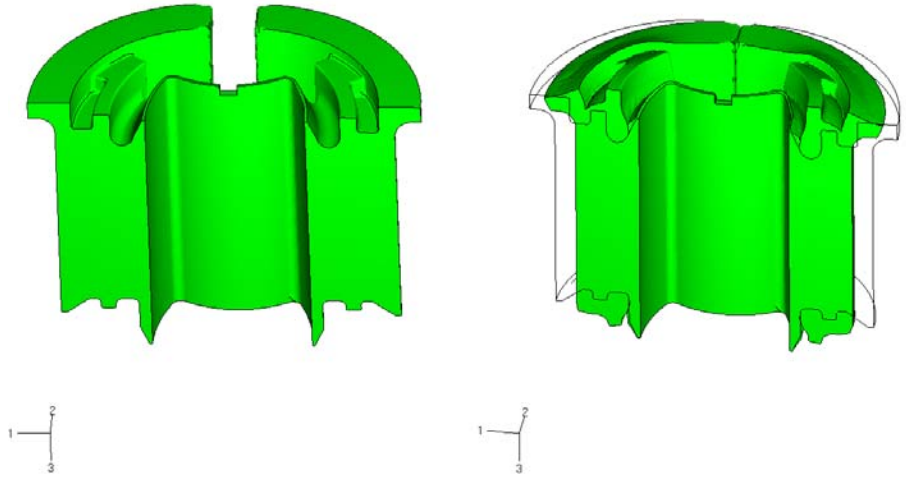

Figure 2. Split shell mount as molded (left) and after assembly (right).

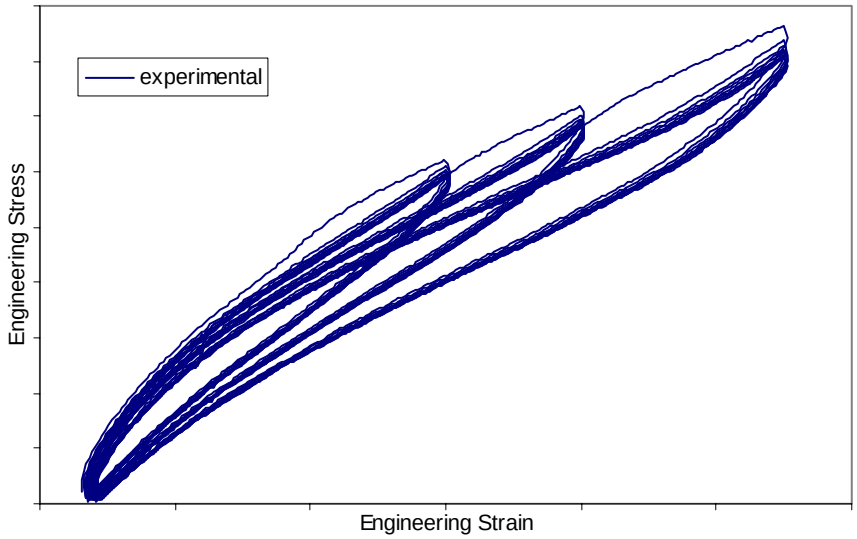

Figure 3. Stress-strain curve obtained under quasi-static cyclic loading. After a few cycles of preconditioning under a given peak strain, the material behavior is approximately hyperelastic. The particular hyperelastic behavior depends on the preconditioning level, however. This dependence is known as the Mullins effect.

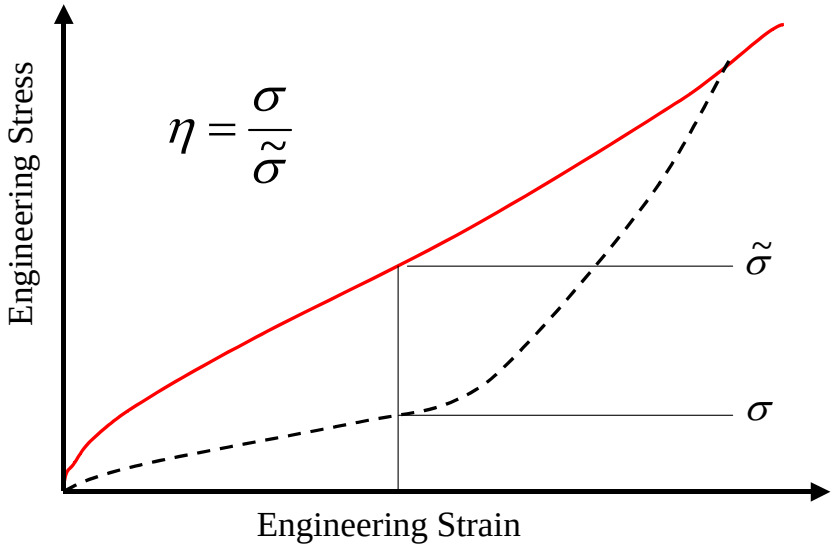

Figure 4. The function η defines the ratio of the preconditioned stress to the stress on the primary curve, at a given state of deformation.

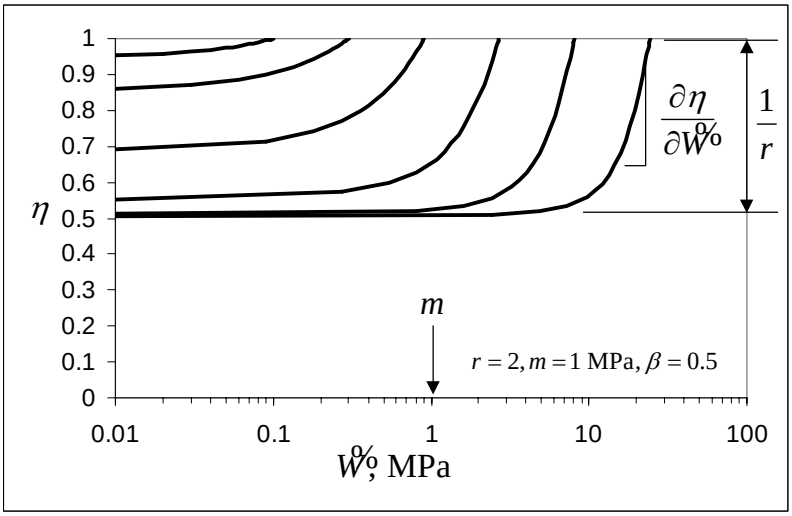

Figure 5. Dependence of the ratio η on instantaneous and max-ever strain energy density on the primary stress-strain curve, for typical values of the material parameters *r*, *m*, and β. The parameter *r* is related to the maximum degree to which the material can soften. The parameter *m* demarcates roughly the minimum max-ever strain energy density $\bar{W}_{\max}$ required to cause the full amount of softening 1/*r*.

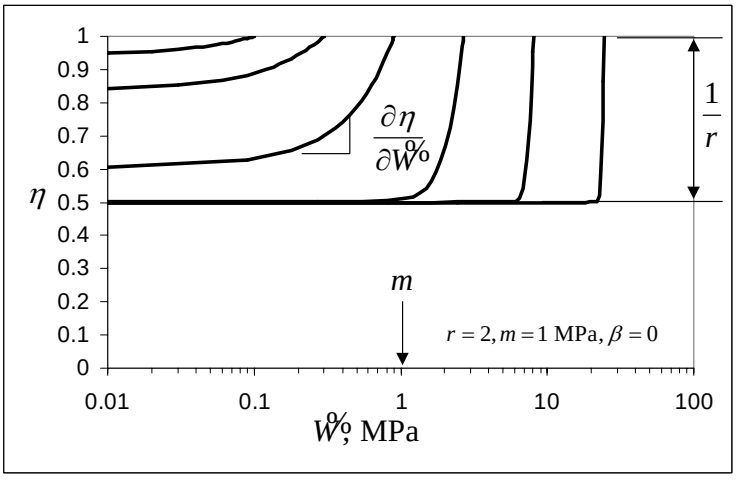

Figure 6. Dependence of the softening ratio η on instantaneous and max-ever strain energy density on the primary stress-strain curve for the original model of Ogden and Roxburgh (ie $\beta = 0$). The sharp change in slope that occurs for large $\bar{W}_{\max}$ when $\bar{W} / \bar{W}_{\max} = 1$ can cause convergence difficulties in a FEA.

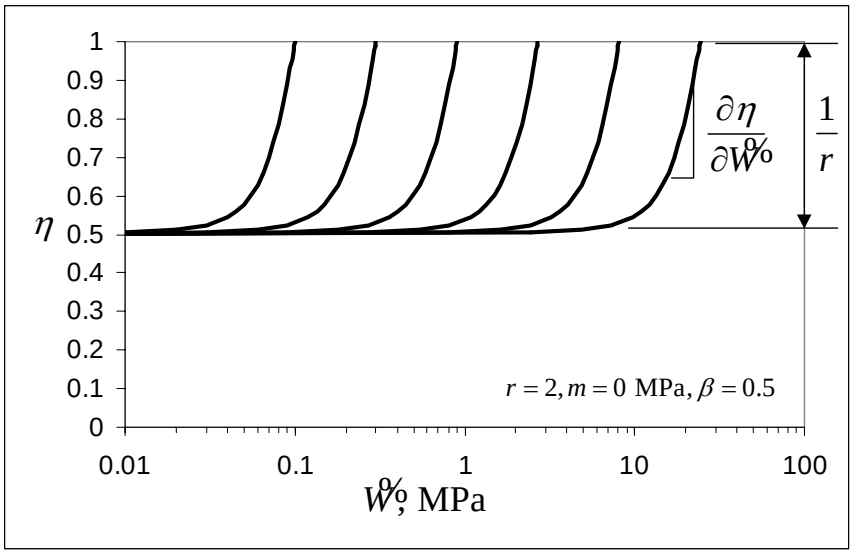

Figure 7. Dependence of the softening ratio η on instantaneous and max-ever strain energy density on the primary stress-strain curve when the parameter *m* is set to zero. When *m* = 0, full softening is predicted to occur at arbitrarily small strains. This behavior is not physically realistic.

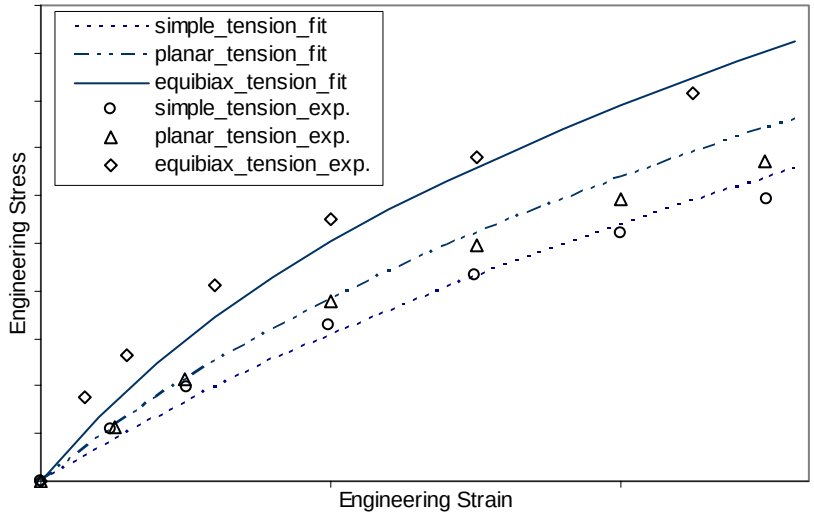

Figure 8. Comparison of Mooney-Rivlin model to monotonic stress-strain results in simple, planar and equibiaxial tension.

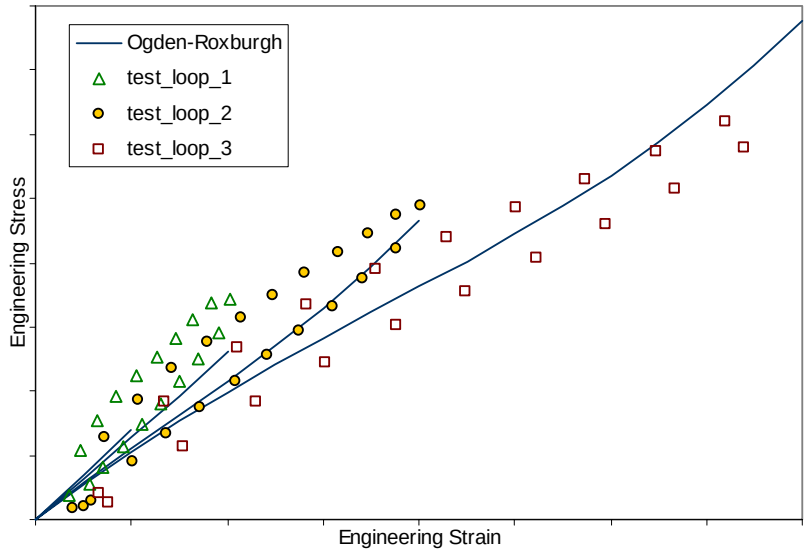

Figure 9. Comparison of stress-strain curves measured following various levels of preconditioning to predictions of the Ogden-Roxburgh model.

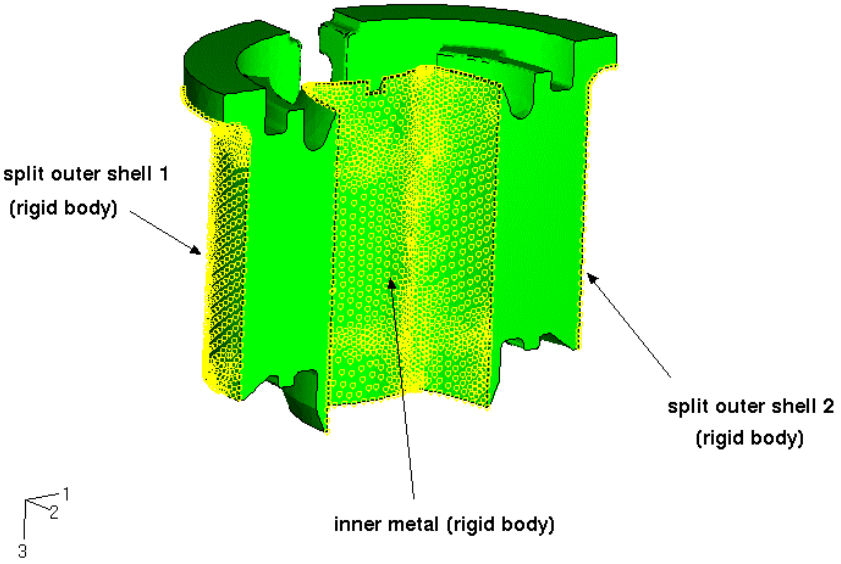

Figure 10. Boundary conditions and model details for split shell mount.

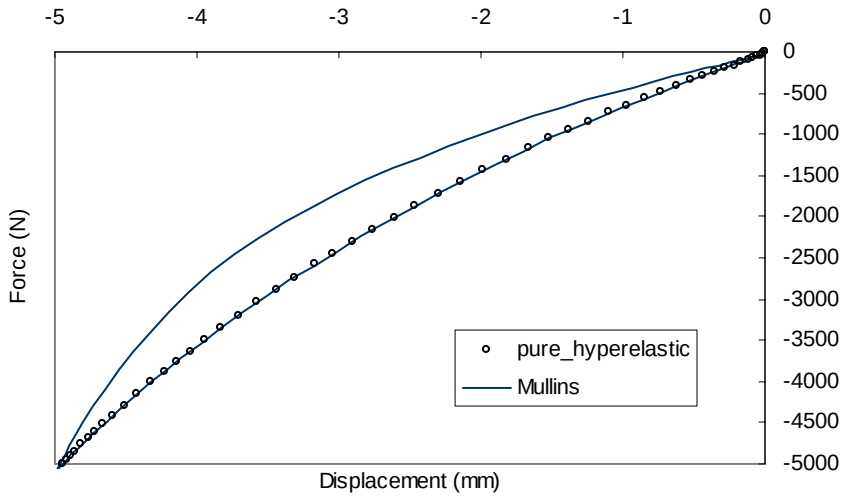

Figure 11. Comparison of predicted load-deflection response for 1/2 of clamshell mount with and without Mullins effect. The component response is similar to the material response.

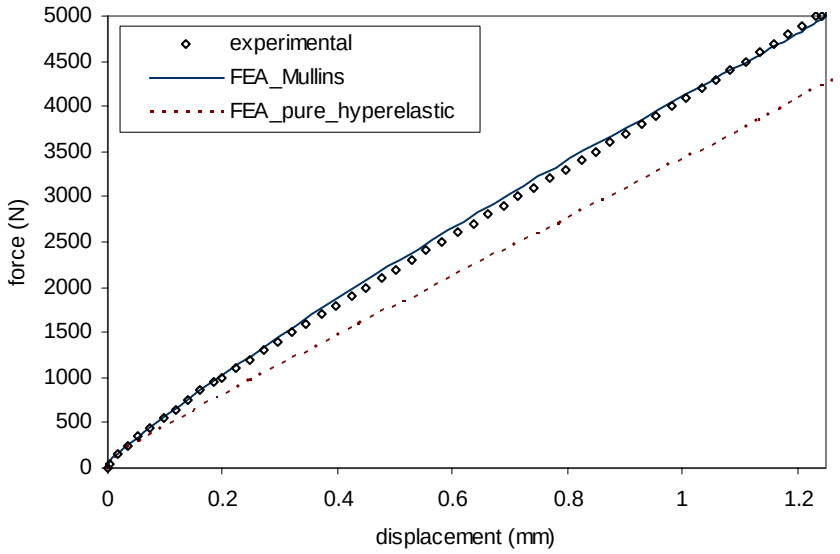

Figure 12. Comparison of predicted load-deflection response for whole split shell mount with and without Mullins effect. The component response has become stiffer due to the difference in pre-conditioning between the two pre-loaded halves of the mount.

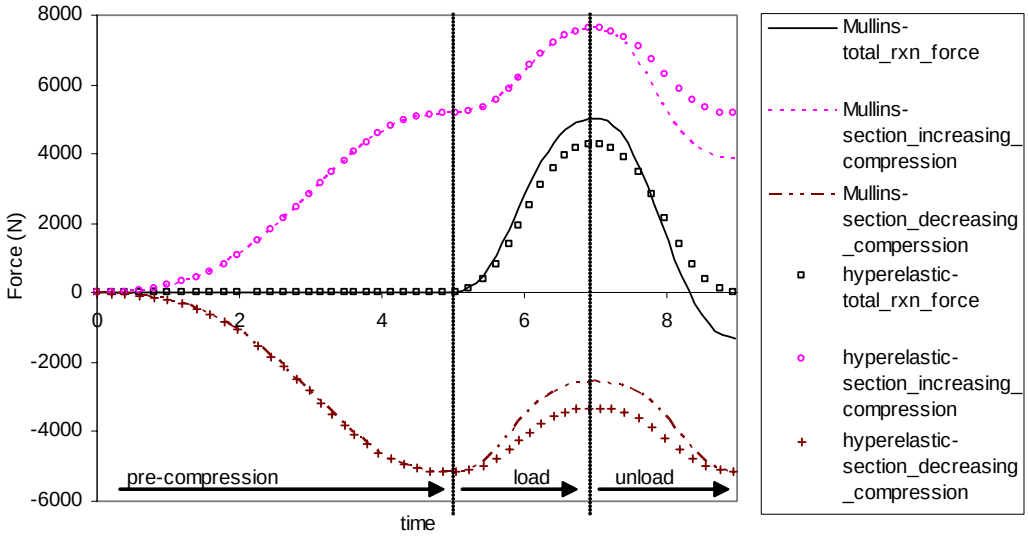

Figure 13. Time history of loading for individual halves of a split shell mount, with and without Mullins effect.

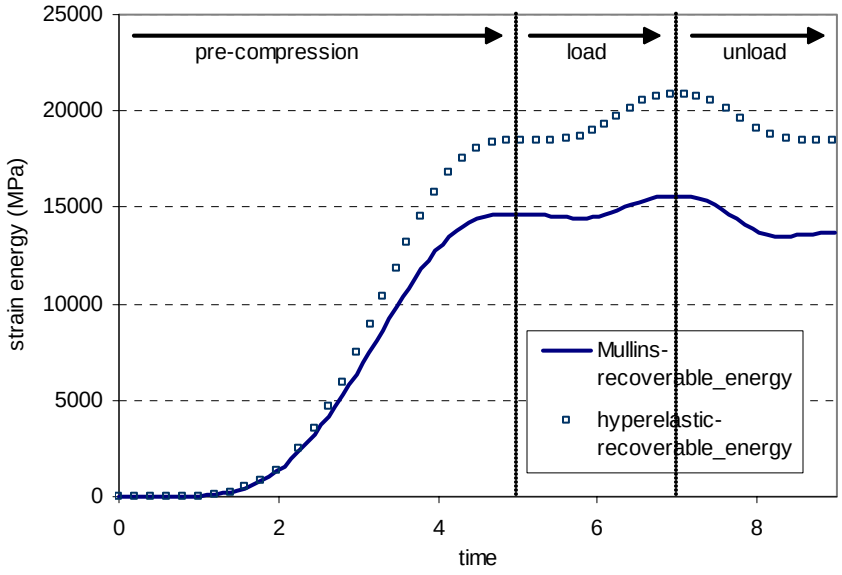

Figure 14. Comparison of the recoverable part of the energy in the whole model.

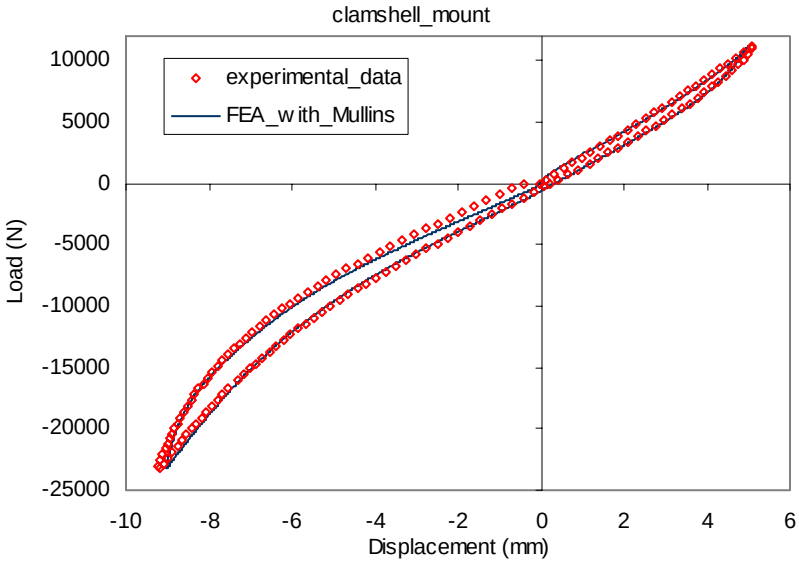

Figure 15. Correlation of FEA with Mullins effect versus experimental data.

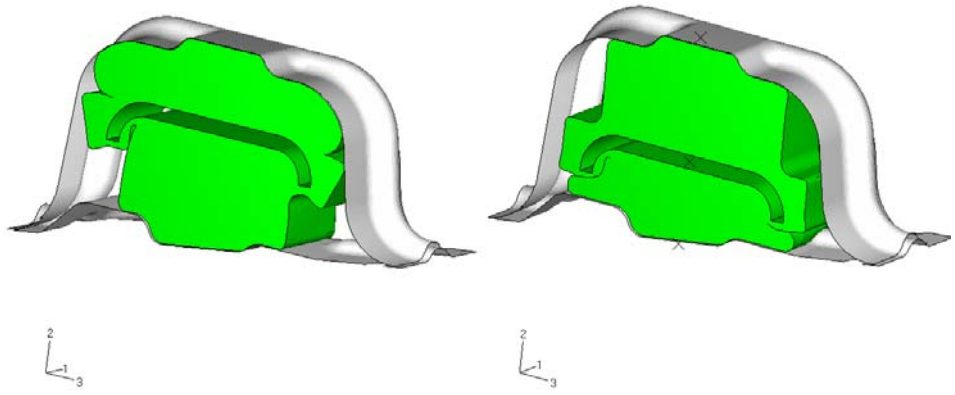

Figure 16. Deformation of clamshell mount rubber element at peak loads.